KFUPM
Journal of Undergraduate Research International

Diamond Open Access

Article
Electrical Engineering/Mechanical Engineering/Physica

Numerical Investigation of a Divided-Leg Thermoelectric Generator for Enhanced Power and Efficiency

Md. Habibur Rahman Aslam, Foyzul Karim, and Anisul Islam Suva*

Cite https://doi.org/10.64589/juri/214391

Submitted: June 2, 2025 **Revised:** July 20, 2025 **Accepted:** November 18, 2025

ABSTRACT

Given the ongoing energy crisis, researchers plus policymakers worldwide are pursuing alternative energy solutions. Thermoelectric generators (TEGs) are an attractive approach offering a sustainable and efficient means to address current energy demands. Despite the numerous TEG designs, their efficiency remains poor, posing a challenge to their widespread adoption. In this study, we introduce a leg-division method designed to enhance the efficiency of TEGs. To establish its superiority, the design was simulated using COMSOL Multiphysics 5.5, and its performance was benchmarked against a conventional rectangular leg geometry. Across the two designs, a temperature gradient of 280 K ($T_h = 573$ K, $T_c = 293$ K) was maintained, and the material volume was held constant to ensure a fair comparison. The results show that the new model achieves an open-circuit voltage of 64.3 mV, which is 1.2 times higher than that of the baseline geometry. The maximum power output reaches 49.22 mW, 2.8 times greater than the conventional model, and the maximum efficiency is 6.69%, indicating 2.1×improvement over the prior geometry. The enhanced performance of the new TEG design has the potential to redefine deployment in renewable energy generation by improving waste heat harvesting, thereby advancing sustainable power generation.

Keywords: thermoelectric generators, divided leg, geometry, energy, COMSOL

1. INTRODUCTION

In recent decades, the world has faced an escalating energy crisis driven by rising demand from urbanization, industrialization, economic growth, and rapid technological development[1]. At the same time, primary energy sources such as hydrocarbon resources are being depleted[2]. Furthermore, the combustion of fossil fuels markedly elevates CO_2 output, contributing to sea-level rise, natural disasters, and global warming[3]. In this context, renewable energy sources provide robust means for tackling these pressing challenges[4]. Thermoelectric generators (TEGs) contribute to solving the energy crisis and mitigating environmental impacts by converting waste heat into electricity and reducing the reliance on fossil fuels, thereby supporting the shift toward renewable and sustainable energy sources[5]. However, their application is limited by their bulk size, low energy conversion efficiency, material costs, and the complexity of thermal management in practical systems[6,7].

Several studies have been conducted to enhance the efficiency of TEGs, which fall into three main approaches. First, improving the thermoelectric material properties[8] to achieve a higher figure of merit (ZT) substantially boosts the performance. Second, segmentation[9] techniques offer higher output power and conversion efficiency than conventional designs. Third, designing novel geometries[10] for the device further enhances the heat transfer and overall efficiency.

Khalil et al. evaluated different geometrical shapes (five shapes: rectangular, I-leg, X-leg, trap-leg, and Y-leg) of the same volume using the finite element method. The study found that a rectangular leg model in a thermoelectric generator with a 6 mm leg length achieved the highest efficiency (5.482%) and output power, outperforming other shapes despite identical volumes[11]. Quan et al.[12] designed a TEG system with a polygonal heat exchanger and sickle-shaped fins to increase waste-heat reclamation. Transient CFD analysis under CLTC conditions showed improved performance, with power rising from 24.48 W to 34.48 W and confirmed fidelity, aiding TEG optimization for automotive use. Luo et al.[13] proposed a novel Y-type TEG configuration that increased the output power and conversion efficiency by 87.5% and 42.62% respectively, at the exhaust temperature of 450 K and velocity of 20 m/s when applying the Y-type design ($\Delta L = 0$ mm) instead of the conventional π-type (or rectangle-shaped) TEG. Ibeagwu et al.[14] studied geometries such as rect-leg, trap-leg, Y-leg, I-leg, and X-leg with varied leg forms and found that the X-leg offers the highest power density. Siddique et al. found that under a constant temperature boundary condition ($\nabla T = 10$ °C), the rectangular TEG produced 1.4 times more power than the trapezoid configuration. However, the power density of the rectangular configuration remains comparable to that of the trapezoidal one[15].

In this study, we investigated the divided-leg geometry within the device to improve its output performance. This innovative design effectively reduces the internal resistance, resulting in an elevated open-circuit voltage, enhanced power generation, and superior energy-conversion efficiency. The notable performance improvements in this structure demonstrate its substantial potential for renewable energy applications, enabling pathways to optimize TEGs in sustainable energy systems. These findings highlight the importance of geometric modifications in advancing thermoelectric technology for practical energy solutions.

Following the general background, the introduction should summarize prior work relevant to the present study[1]. This includes citing earlier results and highlighting the current state of knowledge. Authors should subsequently identify gaps, inconsistencies, or limitations in the literature that justify the need for the present research. For example, while traditional steel dowels have been widely studied, research on small-diameter FRP dowels in real-world applications remains limited[2,3]. Such gaps motivate further investigation and emphasize the originality of the current work. Alvaro et al.[4] found that the bond strength of three different GFRP rebar types—sand-coated, helically grooved, and lugged—varied based on surface enhancement, but was not significantly affected by exposure time or temperature in seawater environments.

Next, the purpose and objectives of the present study should be clearly stated. Authors should define what their research aims to investigate or demonstrate and succinctly outline methods. This creates a coherent bridge from the literature background to the specific contribution of the current paper. A well-defined research objective helps audiences understand the scope and importance of the study.

In some cases, authors may opt to add a final paragraph outlining the structure of the paper, briefly describing what each subsequent section will address. To ensure proper citation and referencing throughout the manuscript, it is strongly advised that authors use reference management software such as Mendeley, Zotero, or EndNote.[5,6]. Zotero was the reference manager employed to manage citations in this document. These tools support the Nature citation style required by the Journal of Undergraduate Research International and streamline the process of formatting in-text citations and the reference list. This section should be focused and concise, typically not exceeding 10% of the total word count of the paper.

2. DIVIDED LEG STRUCTURE

In the leg division method, each TEG leg is divided into two parts—upper and lower—with a metallic conductor incorporated between them, as illustrated in Figure 1a. These segments comprise alternating thermoelectric semiconductors that generate opposite thermoelectric potentials. Specifically, in the left leg of the proposed divided-leg geometry, the upper section contains a p-type semiconductor. Conversely, the lower section is composed of an n-type semiconductor. In p-type semiconductors, holes act as the majority charge carriers; they absorb thermal energy from the hot side and diffuse it toward the central conductor. In contrast, n-type semiconductors have electrons as the majority charge carriers, which diffuse toward the cold side. This movement results in effective hole diffusion toward the central conductor, establishing a thermoelectric potential across the leg. Thus, a positive potential develops at the central conductor of the left leg owing to the directional movement of the charge carriers. Similarly, the right leg of Figure 1a comprises an n-type semiconductor in the upper part and a p-type semiconductor in the lower part, resulting in the development of a negative potential at the central conductor. These two central conductors function as the electrical terminals of the divided-leg geometry, enabling connection to the external circuit.

Moreover, the conductor at the center serves dual roles: it acts as both an electrical junction and a thermal interface. This structure limits Joule heating and enables more efficient thermoelectric conversion by allowing localized charge separation and shorter diffusion paths for charge carriers. This design strategy is especially beneficial for microscale or densely packed TEG systems, where resistive losses can significantly affect overall performance.

The equivalent circuit diagrams for the divided-leg geometry and the rectangular leg are shown in Figure 2 a and b, respectively.

Each semiconductor (p or n), conductor, and soldering junction has its own internal resistance, denoted as R_P or R_N, R_C, and R_{Sh}. The total internal resistance of the system is obtained by

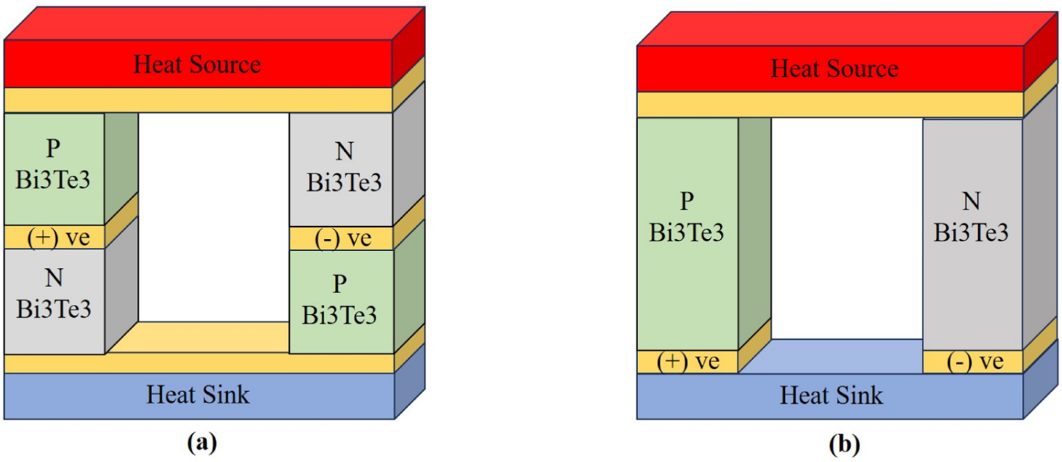

Figure 1. Schematic diagram of (a) divided-leg geometry, (b) rectangular leg geometry

summing component values. Equivalent circuit diagrams for the divided-leg and rectangular-leg geometries appear in Figure 2 (a) and (b), respectively.

The basic relationship of electrical resistance is given by the following equation:

$$R = \frac{l}{\sigma A} \tag{1}$$

where R is the resistance, l is the length of the conductor, σ is the electrical conductivity, and A is the cross-sectional area. Considering that the copper conductor resistance (R_C) and soldering resistance (R_{Sh}) are negligible, the equivalent internal resistance of the rectangular TEG is:

$$R_{REC} = R_P + R_N \tag{2}$$

where R_P and R_N denote the resistances of the p- and n-type legs, respectively.

In a divided-leg geometry, shortening the effective electrical path within each material segment by splitting them into equal upper and lower halves reduces the resistive losses, enhances the current flow, and improves the voltage output. Each leg forms two branches (p- and n-type) and two parallel branches, each consisting of $R_P/2$ and $R_N/2$ in series. Because the electrical resistance in parallel pathways combines inversely, this geometry effectively reduces the total internal resistance of the TEG to approximately one-fourth of that in a conventional series-connected rectangular leg design. Thus, a reduction in the internal resistance occurs in the leg division geometry owing to the parallel configuration.

Thus, the total internal resistance in this configuration can be written as:

$$R_{REC} = \frac{R_P + R_N}{4} \tag{3}$$

Although the equivalent circuit diagrams in Figure 2 explicitly include R_C and R_{Sh}, these components are considered negligible in the analytical simplification to streamline the resistance calculations. While this is a common assumption because of their typically low values relative to the semiconductor resistance, notably, neglecting R_C and R_{Sh} may introduce minor deviations in precise modeling, especially in high-precision or miniaturized TEG systems.

This reduction in the internal resistance reduces dissipation, allowing higher current flow and improving the voltage output, thereby enhancing the overall power generation efficiency of the thermoelectric generator.

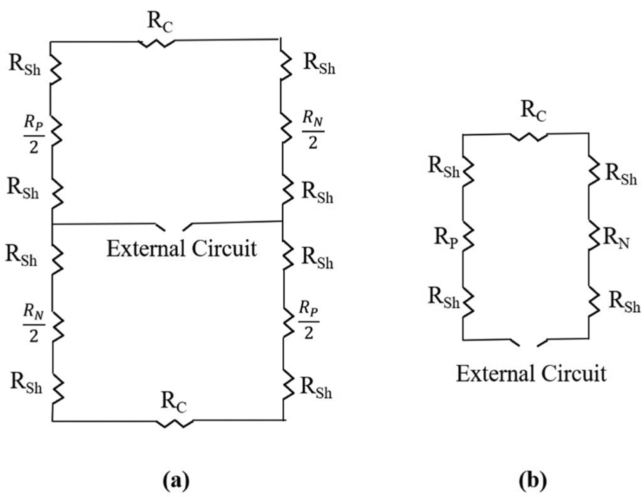

Figure 2. Circuit diagram of (a) divided-leg geometry, (b) rectangular leg geometry

3. SIMULATION

Both TEG models were simulated using COMSOL Multiphysics 5.5 by integrating the Heat Transfer and AC/DC modules to resolve their thermal and electrical characteristics. The Heat Transfer module modeled the temperature distribution and heat flow, whereas the AC/DC module solved the electrical potential and current flow. This coupled approach is critical for evaluating thermoelectric performance under realistic operating conditions. In these simulations, the heat source temperature was fixed at 573 K, and the heat sink temperature was set to 293 K.

3.1. Necessary Equations of Simulation.

Energy flows as heat from the hot side and is absorbed by thermoelectric materials, as governed by conservation of energy:

$$\rho C_{p.} u \nabla T + \nabla q = Q + Q_{ted} \tag{4}$$

where ∇q would represent the divergence of the heat flux vector, and Heat flux, $q = -k.\nabla T$

This equation describes the conductive heat transfer and includes thermoelectric heat sources, including the Joule and Peltier effects.

The electric current interface models current conservation based on Ohm's law, using the scalar electric potential as the primary variable. This enables the computation of the electric potential, current density, and electric field within the conductive materials.

$$\nabla J = Q_j \tag{5}$$

$$J = \sigma E + J_e \tag{6}$$

$$E = -\nabla V \tag{7}$$

These equations capture the response of electrical currents to electric fields and external sources within the material. This multiphysics interface combines electric currents and heat transfer in solid modules, enabling the simulation of the interrelated Peltier, Seebeck, and Thomson effects in thermoelectric devices.

$$Q = P.J \tag{8}$$

$$P = S.T \tag{9}$$

$$J_e = -\sigma S \nabla T \tag{10}$$

Nomenclature:

C_p – Heat capacity (J/kg.K)
J – Induced current density
ρ – Material density (kg/m^3)
J_e – External current density
T – Temperature (K)
Q_j – Current source
Q – Volumetric heat generation from internal sources (W/m^3)
k – Thermal conductivity

Q_{ted} – Thermoelectric heat source or sink associated with the Thomson and Peltier effects (W/m^3)
σ – Electrical conductivity
P – Peltier Coefficient
h – Convective heat transfer coefficient
α – Seebeck coefficient
ΔT – Temperature difference
E – Electric field
V – Electric potential
ZT – Dimensionless figure of merit

3.2. Materials. To compare the performance of both models, Bismuth Telluride (Bi_2Te_3) was used as the thermoelectric material. The Seebeck coefficient, electrical conductivity, and thermal conductivity were the primary thermoelectric properties evaluated. The properties of Bi_2Te_3 appear in Table 1.

Ceramic (Al_2O_3) was used as the hot- and cold-side material because of its excellent thermal stability, high-temperature resistance, and low thermal expansion, which make it ideal for maintaining structural integrity during thermal cycling. Copper was chosen as the conductor because of its high electrical and thermal conductivities, which ensure minimal resistive losses and efficient heat transfer. For both models, the cross-sectional area was set to 1 mm^2 and the total length to 2.5 mm.

4. RESULTS AND DISCUSSION

The performance of the TEG was evaluated using key metrics: the open-circuit voltage, load terminal voltage, load current, output power, and energy conversion efficiency. The geometrical structure of the TEG strongly affects these parameters. A comparison of these parameters between the two models demonstrates the validity of the proposed design.

4.1. Thermal and Voltage Distribution. Figure 3 a and b show the simulated thermal distributions for the proposed divided-leg geometry and conventional rectangular leg geometry, respectively. In both models, a temperature gradient of 280 K was imposed, with the hot side maintained at 573 K and the cold side maintained at 293 K. However, the divided-leg geometry ensures slightly improved thermal utilization by reducing the localized thermal resistance at the conductor junction, facilitating efficient heat transfer through the thermoelectric materials. Although the overall thermal profiles appear similar, the performance enhancement in the divided-leg design mainly arises from its lower internal resistance and optimized electrical configuration rather than from a significant difference in temperature distribution.

Table 1. *Temperature-Dependent Material Properties[16] of Bi_2Te_3*

Temperature (K)	Seebeck Coefficient (μ V/K)	Thermal Conductiviy (W/mK)	Electrical Conductivity (S/m)
200	168	2.4	1.4286×10^5
250	192	1.9	1.1111×10^5
300	210	1.6	0.86957×10^5
350	225	1.6	0.71429×10^5
400	237	1.75	0.58824×10^5

The potential developed at the terminal of the divided-leg geometry is 64.3 mV, as shown in Figure 3 (c), while the conventional rectangular-shaped geometry generates a terminal potential of 54 V, as shown in Figure 3 (d). The COMSOL simulation confirms that the divided-leg geometry not only improved heat distribution but also enhanced voltage development, demonstrating superior performance for thermoelectric energy conversion.

4.2. Load Current and Terminal Voltage. When a load is connected between the two terminals of the TEG, current flows through the load. The magnitude of the current can be determined via Ohm's law.

$$I = \frac{V}{R_L + R_{int}} \tag{11}$$

Additionally, the internal resistance of the device causes a voltage drop that reduces the available terminal voltage at the load. The load-end TEG voltage is given by

$$V = \frac{R_L \times V_{OC}}{R_L + R_{int}} \tag{12}$$

Figure 4 (a) shows that the divided-leg geometry consistently yields a higher current than the rectangular geometry, particularly at lower resistances. Additionally, the divided-leg geometry again outperforms, maintaining a higher voltage across the range, with the gap most noticeable at lower resistances, as shown in Figure 4 (b). Both graphs highlight the greater electrical efficiency of the divided-leg geometry. Elevated current enhances the power output and improves the energy delivery to low-resistance loads, making the TEG more suitable for practical applications. A higher terminal voltage reduces the transmission losses, enhances interfacing to commercial electronics, and facilitates their integration into external circuits. Together, the high current and voltage optimize the power efficiency, increase the system flexibility, and expand the operational range of the TEG, making it more effective for energy harvesting and remote power generation.

4.3. Power. This current flow generates power at the load terminals, representing the usable output power. This power is computed using the following equation:

$$P = I^2 R_L \tag{13}$$

The graph in Figure 5 shows the power developed for both the divided-leg geometry and the rectangular TEG. The divided-leg geometry achieves a maximum power output of 49.22 mW, significantly outperforming the rectangular leg shape, which yields 17.36 mW under identical conditions.

Rectangular leg geometry is commonly used owing to its structural simplicity and reliability[11,15]. Several recent studies have demonstrated that modified geometries can significantly improve the performance of TEGs. Siddique et al.[15] found that for a given restricted volume envelope, the trapezoidal-shaped TE prototype generates 1.24 times more voltage and 1.5 times more power when compared to the rectangular-shaped prototype at 30 °C hot side temperature when the cold side is exposed to the surroundings. Okirigiti et al.[17] reported that the trapezoidal-shaped legs-TEG with a top surface area of 2.5 × 2.5 mm^2 converts the

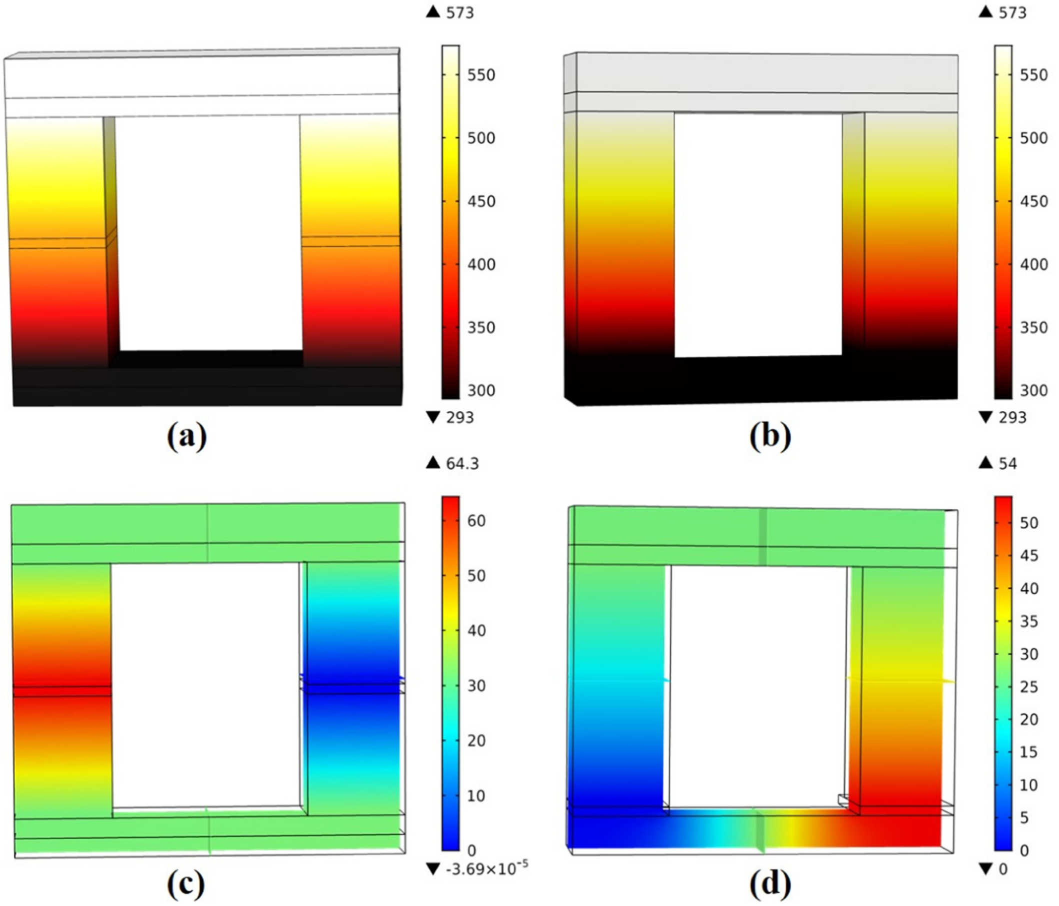

Figure 3. Thermal Distribution of divided-leg geometry, (b) Thermal Distribution of rectangular leg geometry, (c) Voltage Distribution of divided-leg geometry, (d) Voltage Distribution of rectangular leg geometry

output power of 0.60 mW from a temperature gradient (ΔT) of 200 K, which represents a two-fold increase compared to the cuboid-shaped legs (5×5 mm^2)-based TEG. Yin et al.[18], conducted a comparison-based study between the developed T-shaped and the conventional π-shaped TEGs, and reported that the specific output power was significantly increased by 90.1% under the same given thermal conditions.

Compared with existing geometric configurations, the proposed divided-leg design yields a 2.8-fold increase in the power output, outperforming all previously reported modifications. This significant enhancement underscores the superior efficacy of divided-leg geometry. Elevated power output in TEGs is critical because it directly improves the energy conversion efficiency, thereby facilitating more effective utilization of waste heat in sustainable power generation applications, including industrial processes and renewable energy systems.

4.4. Efficiency. Electrical power is the transduction of heat energy absorbed from a heat source. The amount of absorbed heat energy is calculated using the following equation:

$$Q_h = \alpha T_h I - 0.5(I^2 R_{int}) + K(T_h - T_c) \tag{14}$$

where, $\alpha = \alpha_p - \alpha_n$, $K = \frac{k_p A_p}{L_p} + \frac{k_n A_n}{L_n}$, R_{int} = internal resistance, I = current flow.

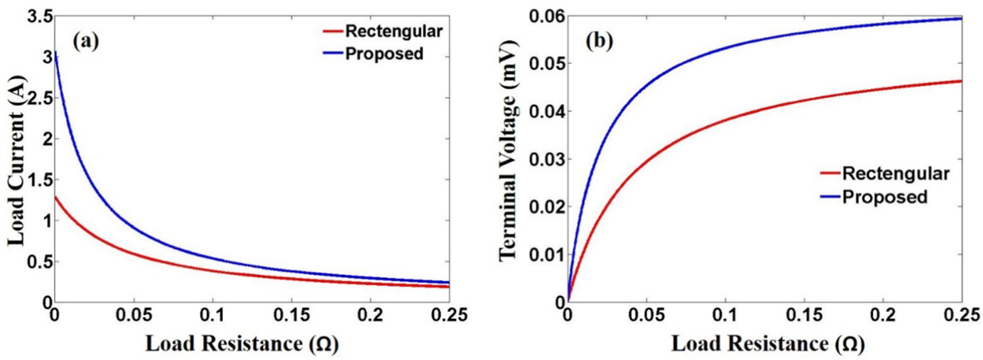

Figure 4. Graph of (a) Load Current (A) vs Load Resistance (Ω), (b) Load terminal voltage (mV) vs Load Resistance (Ω)

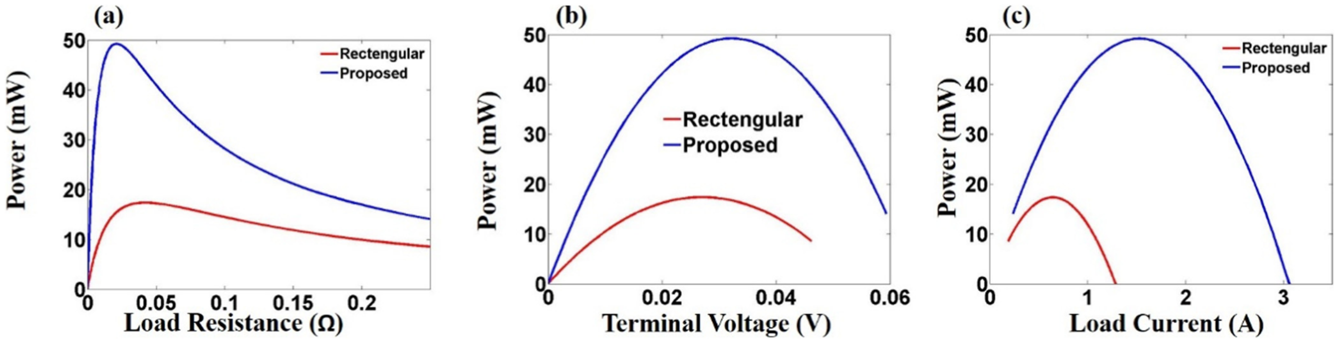

Figure 5. Graphs of (a) power vs. Load Resistance, (b) power vs. terminal voltage, and (c) power vs. load current

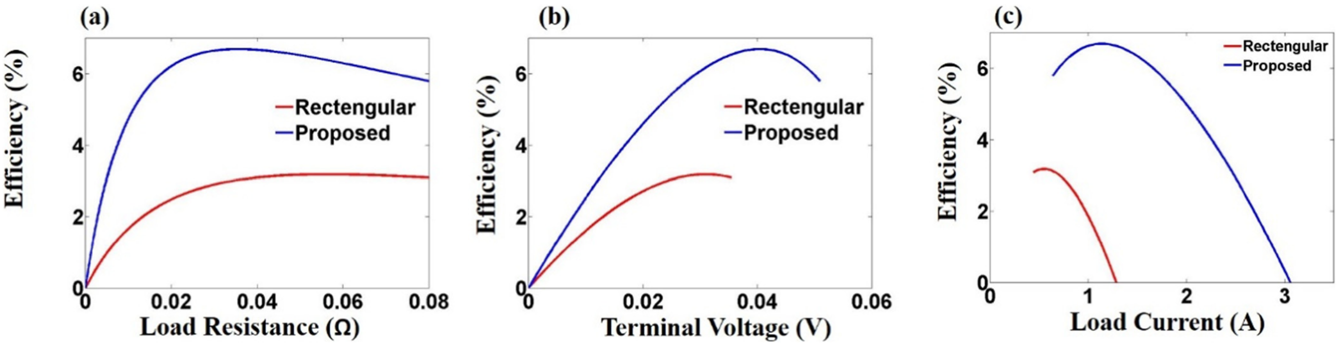

Figure 6. Graphs of (a) efficiency vs. load resistance, (b) efficiency vs. terminal voltage, and (c) efficiency vs. load current

The efficiency of this energy conversion process is given as the ratio of the output electrical power to the absorbed heat energy.

$$\eta = \frac{P}{Q_h} \tag{15}$$

High efficiency in TEGs is vital because it maximizes the energy conversion from heat to electricity, enhancing practicality, material efficiency, and overall performance. Figure 6 shows the efficiency variations of the proposed TEG unit under different operating conditions. The graph demonstrates that the rectangular leg geometry achieves a maximum efficiency of 3.18%, whereas that of the proposed divided-leg geometry reached 6.69%.

Several recent studies have highlighted the influence of leg geometry on device performance. Khalil et al.[11] found that among five geometries of equal volume, the rectangular leg attained the highest efficiency (5.482%). Chen et al.[19] introduced a cylindrical TEG incorporating hot-side shunts and an optimized heat exchanger with segmented fin-hollow channels. By adjusting the blocking plate location and fin-to-hollow height ratio, they obtained a 108.8% increase in power and a 72.8% efficiency gain with optimal performance at moderate exhaust velocities, thereby guiding future TEG designs.

However, the present work demonstrates that the proposed divided-leg geometry achieves over a two-fold improvement in maximum efficiency. This substantial improvement highlights the advantages of the divided-leg geometry, including reduced internal resistance, enhanced current flow, and improved thermal gradient utilization. Higher efficiency not only boosts the electrical output of TEGs but also improves practicality for energy harvesting applications, particularly in waste heat recovery and remote power generation.

5. CONCLUSION

The newly proposed divided-leg geometry exhibited greater thermoelectric efficacy. For a temperature gradient of $\Delta T = 280$ K (Th = 573 K, Tc = 293 K), the traditional rectangular leg structure yielded an open-circuit voltage of 54 mV, while the divided-leg geometry achieved 64.3 mV. Additionally, this divided-leg design produced a maximum power output of 49.22 mW, compared to just 17.36 mW for the rectangular geometry. Consequently, the energy conversion efficiency of the divided-leg geometry reached approximately 6.69%, significantly outperforming the 3.18% efficiency of the traditional design. These results highlight the high potential and practical viability of the divided-leg geometry, offering a promising solution for improving TEG performance. These improvements make the divided-leg geometry a promising candidate for applications in wearable electronics, vehicle exhaust heat recovery, and remote power sources.

AFFILIATIONS AND AUTHOR DETAILS

Undergraduate Authors

Md. Habibur Rahman Aslam – *Department of Electrical and Electronic Engineering, Chittagong University of Engineering & Technology (CUET), Chattogram, Bangladesh;* 0009-0008-0751-9645
Email: u1902135@student.cuet.ac.bd

Foyzul Karim – *Department of Electrical and Electronic Engineering, Chittagong University of Engineering & Technology (CUET), Chattogram, Bangladesh;* 0009-0007-8318-0519
Email: u1902169@student.cuet.ac.bd

Corresponding Author

Anisul Islam Suva – *Research Mentor, Institute of Energy Technology, Chittagong University of Engineering & Technology (CUET), Chattogram, Bangladesh;* 0009-0000-7967-7548
Email: anisulislam.me@cuet.ac.bd

ACKNOWLEDGEMENTS

The authors acknowledge the support and resources from COMSOL. Extensive user forums, tutorials, and shared simulation insights enabled the modeling and validation processes in this study. The collaborative knowledge base offered by COMSOL users worldwide has materially aided in overcoming technical challenges and improving simulation accuracy.

CONFLICTS OF INTEREST

The authors declare no conflicts of interest regarding the publication of this manuscript.

FINANCIAL DISCLOSURE

The authors received no specific funding for this work.

REFERENCES

(1) Gajdzik, Bożena, et al. "The influence of the global energy crisis on energy efficiency: A comprehensive analysis." *Energies* 17.4 (2024): 947.

(2) Höök, Mikael, and Xu Tang. "Depletion of fossil fuels and anthropogenic climate change—A review." *Energy policy* 52 (2013): 797–809.

(3) Fang, JingYun, et al. "Global warming, human-induced carbon emissions, and their uncertainties." *Science China Earth Sciences* 54 (2011): 1458–1468.

(4) Poudyal, Ramhari, et al. "Mitigating the current energy crisis in Nepal with renewable energy sources." *Renewable and Sustainable Energy Reviews* 116 (2019): 109388.

(5) Mamur, Hayati, et al. "Thermoelectric generators act as renewable energy sources." *Cleaner Materials* 2 (2021): 100030.

(6) Chen, Jinlong, et al. "Enhanced efficiency of thermoelectric generator by optimizing mechanical and electrical structures." *Energies* 10.9 (2017): 1329. (6)

(7) Khan, Salman, et al. "High power density of radiative-cooled compact thermoelectric generator based on body heat harvesting." Nano Energy 87 (2021): 106180. (7)

(8) He, Hailong, et al. "Comprehensive modeling for geometric optimization of a thermoelectric generator module." *Energy conversion and management* 183 (2019): 645–659.

(9) Yang, Wenlong, et al. "Joint optimization of leg configuration and fin structure in a two-stage segmented thermoelectric generator for enhanced 3E performance." *Applied Thermal Engineering* 271 (2025): 126354.

(10) Schilz, J., et al. "A local selection criterion for the composition of graded thermoelectric generators." *Journal of applied physics* 83.2 (1998): 1150–1152.

(11) Khalil, ALkhadher, et al. "Performance comparison of TEGs for diverse variable leg geometry with the same leg volume." *Energy* 224 (2021): 119967.

(12) Quan, Rui, et al. "Dynamic performance of a polygonal thermoelectric generator using sickle-shaped fins for automotive application." *Applied Thermal Engineering* 255 (2024): 123985.

(13) Luo, Ding, et al. "A novel Y-type thermoelectric generator configuration for the fluid waste heat recovery." *Applied Thermal Engineering* 270 (2025): 126226.

(14) Ibeagwu, Onyebuchi Isreal. "Modelling and comprehensive analysis of TEGs with diverse variable leg geometry." *Energy* 180 (2019): 90–106.

(15) Siddique, Abu Raihan Mohammad, Shohel Mahmud, and Bill Van Heyst. "Performance comparison between rectangular and trapezoidal-shaped thermoelectric legs manufactured by a dispenser printing technique." *Energy* 196 (2020): 117089.

(16) Prasad, Asutosh, and Raj CN Thiagarajan. "Multiphysics modeling and multilevel optimization of thermoelectric generator for waste heat recovery." *Proceedings of the COMSOL Conference*. 2018.

(17) Okirigiti, Momanyi Amos, et al. "Enhanced energy harvesting performance of bendable thermoelectric generator enabled by trapezoidal-shaped legs." *Journal of Power Sources* 631 (2025): 236254.

(18) Yin, Tao, et al. "Performance analysis and design optimization of a compact thermoelectric generator with T-Shaped configuration." *Energy* 229 (2021): 120652.

(19) Chen, Jie, et al. "Innovative design and numerical optimization of a cylindrical thermoelectric generator for vehicle waste heat recovery." *Energy Conversion and Management* 326 (2025): 119478.